Electronic Supplementary Information

In-situ Hard Templating Assisted Facet Engineered Two-Dimensional Non-van der Waals $CuInS_2$ for Efficient CO_2 Reduction Reaction

*Shuvojit Mandal[a], Krishnendu Roy[a], Yatendra S. Chaudhary[c] and Praveen Kumar[a,b,]**

[a] School of Materials Science, Indian Association for the Cultivation of Science, Kolkata-700032, India;

[b]Plaksha University, Sahibzada Ajit Singh Nagar, Mohali-140306, India

[c]Materials Chemistry Department, CSIR-Institute of Minerals and Materials Technology, Bhubaneswar-751013, India;

*Corresponding Author Email: praveen.kumar@plaksha.edu.in

Experimental Section:

Specifications of chemicals:

Red Phosphorus (≥99.99%), CuI (≥99.5%), $In(OAc)_3$ (99.99%), Oleylamine (OLM) (≥98%), 1-Octadecene (ODE) (≥99%), Dodecanethiol (DDT) (≥98%), triphenylphosphine (PPh_3) (99%) and DMSO (99.9%) are bought from Sigma Aldrich. $KHCO_3$ (≥99.95%), Formic acid (98-100%) and Isopropanol (≥98%) are bought from Merck. Toray Carbon paper (TGP-H-60, 19×19 cm) is bought from Alfa Aesar. All the chemicals and materials are used as received without further treatment. White Phosphorus is synthesized from Red Phosphorus. All the aqueous solutions are made with Merck water. Ultra-high pure, 99.999% CO_2 and N_2 are supplied by IRS.

Synthesis:

- **Synthesis of White P:**

3 g of red P is vacuum sealed in a quartz tube and horizontally placed inside a tube furnace. It was heated at 600 °C for 3 h and allowed to cool down. The transparent and pale yellowish solid condensed in the opposite side of the quartz tube is collected very cautiously under cold water and preserved under water for further use. Rest impure and unreacted part is deactivated in an open place before discarding.

- **Synthesis of CIPS intermediate:**

0.2 mMol (58.392 mg) $In(OAc)_3$, 0.2 mMol (38.09 mg) CuI and 20 mg (>>0.1 mMol) white Phosphorus (little excess) are taken in a 25 ml 3-neck round bottom flask with 12 ml Octadecene (ODE). Reflux condenser is attached and N_2 gas is purged inside the flask to make an inert atmosphere inside. Meanwhile, temperature is taken to 100 °C and kept for 1 h so that any undesired gas, volatile impurities or moisture get escaped. Then, gas purging is stopped and made air tight. After that, the reaction medium is heated to 225 °C for 4 h. When the solution turns to black from yellow, 1 ml dodecanethiol is injected and kept in the same temperature for another 3 h. Finally, the reaction is stopped and kept overnight with stirring. The black solid precipitate is collected and washed thoroughly with hexane and ethanol several times with the help of centrifuge. Collected sample is vacuum dried and kept inside a desiccator in vacuum condition.

- **Synthesis of P-doped CIS:**

0.2 mMol (58.392 mg) $In(OAc)_3$, 0.2 mMol (38.09 mg) CuI and 20 mg (>>0.1 mMol) white Phosphorus (little excess) are taken in a 25 ml 3-neck round bottom flask with 12ml Octadecene (ODE). Reflux condenser is attached and N_2 gas is purged inside the flask to make an inert

atmosphere. Meanwhile temperature is taken to 100 °C and kept for 1 h so that any undesired gas, volatile impurities or moisture get escaped. Then, gas purging is stopped and made air tight. After that, the reaction medium is heated to 225 °C for 4 h. When the solution turns to black from yellow, 1 ml dodecanethiol is injected and temperature is taken rapidly to 290 °C and kept for another 3 h. Then reaction is stopped and kept overnight. Finally, the black solid precipitate is collected and washed thoroughly with hexane and ethanol several times with the help of centrifuge. Collected sample is vacuum dried and kept inside a desiccator in vacuum condition.

#Failed attempts:

Instead of white P, we had used large excess triphenyl phosphine and reaction temperature is taken as high as 315 °C but no P incorporation is observed as found from XRD and TEM-EDX in both ODE and OLM solvent. We further used red P directly but then also similar phenomena occurred. This failure led us to use white phosphorus.

We further found that in OLM solvent, white phosphorus reacts and converts to red phosphorus. These failures finally take us to the previous mention synthesis method.

- **Synthesis of Zincblende-CIS:**

0.2 mMol (58.392 mg) $In(OAc)_3$ and 0.2 mMol (38.09 mg) CuI is taken in a 25 ml 3-neck round bottom flask with 12 ml Octadecene (ODE). Reflux condenser is attached and N_2 gas is purged inside the flask to make an inert atmosphere. Meanwhile temperature is taken to 100 °C and kept for 1 h so that any undesired gas, volatile impurities or moisture get escaped. Then, gas purging is stopped and made air tight. After that, 1 ml dodecanethiol is injected and heated to 220 °C for 6 h. Then reaction is stopped and kept overnight. Finally, the black solid precipitate is collected and

washed thoroughly with hexane and ethanol several times with the help of centrifuge. Collected sample is vacuum dried and kept inside a desiccator in vacuum condition.

- **Synthesis of Wurtzite-CIS:**

0.2 mMol (58.392 mg) $In(OAc)_3$ and 0.2 mMol (38.09 mg) CuI is taken in a 25 ml 3-neck round bottom flask with 12ml Oleylamine (OLM). Reflux condenser is attached and N_2 gas is purged inside the flask to make an inert atmosphere. Meanwhile, temperature is taken to 100 °C and kept for 1 h so that any undesired gas, volatile impurities or moisture get escaped. Then, gas purging is stopped and made air tight. After that, 1 ml dodecanethiol is injected and heated to 245 °C for 6 h. Then reaction is stopped and kept overnight. Finally, the black solid precipitate is collected and washed thoroughly with hexane and ethanol several times with the help of centrifuge. Collected sample is vacuum dried and kept inside a desiccator in vacuum condition.

Electrode preparation: All the electrodes are prepared on carbon fiber paper and catalyst ink is drop casted cautiously on both sides of a carbon strip with 0.5×1 cm^2 area so that considering both sides, the final active electrode surface area becomes 1 cm^2. All the samples are dispersed in 300 µl IPA without any binding agent like Nafion solution and sonicated for 20 minutes before drop casting. We have optimized mass loading of P-doped CIS by taking chronoamperometry at -0.84 V_{RHE} with 2 mg, 3 mg and 4 mg catalyst loading for 1 h. We found 3 mg catalyst loading gives highest formate partial current density. We kept catalyst loading fixed to 3 mg also fixed geometrical surface area for all other electrodes to normalize the comparison.

Measurement technique:

X-ray diffraction (XRD) was performed on the Rigaku SmartLab X-ray diffractometer where Cu-Kα was the source. Field emission gun scanning electron microscopy (FE-SEM) (JEOL JSM-7500F), Atomic Force Microscopy (AFM) (Asylum Research MFP-3D using AC160TS silicon probes) in tapping mode and field emission gun transmission electron microscopy (FEG-TEM) (JEOL, JEM 2100F) were used for the characterization of surface morphology, Particle height profile, elemental analysis and further AFM images are processed with WSxM 5.0 and TEM images with the help of Gatan Digital Micrograph software. Omicron Nano-technology X-ray photoelectron spectroscopy (XPS) was used to analyze the oxidation state and surrounding electronic environment.

Electrochemical Measurement technique:

The performance of the electrodes is assessed via an electrochemical workstation (Bio-Logic Science Instruments, Model SP-300/240). LSV and CA are measured in three-electrode modes with Pt mesh as a counter electrode and Ag/AgCl as a reference electrode (CH Instruments) in a customized H-type cell. LSV presented in the main text, is obtained at 20 mV/s scan rate. CO_2 saturated 0.5 M $KHCO_3$ aqueous electrolyte with pH=7.4, is used for all the measurements. All potentials are reported here with respect to Reversible Hydrogen Electrode (RHE) is converted via the following equation –

$$E\ (\text{vs RHE}) = E\ (\text{vs Ag/AgCl}) + 0.222\ \text{V} + 0.059\ \text{V} \times \text{pH}$$

The gas product is analyzed with a GC analyzer (TRACE 1110, Thermo Scientific) after 15 min chronoamperometry at different potential in CO_2 saturated electrolyte inside an air-tight cell and the head space gas is injected in an offline GC via a gas-tight syringe. Standardization curve is

made with standard gas mixture is shown in **Figure S13b**. Faradaic Efficiency is calculated from the following equation-

$$FE_{CO}(\%) = \frac{Q_{CO}}{Q_{total}} \times 100\% = \frac{n_{CO} \times N \times F}{j \times t} \times 100\%$$

Where, n_{CO} is the amount of formate produced, N is the number of electrons transferred (2 for CO), and F is the Faradaic constant.

We analyzed the Liquid product after 1 h Chronoamperometry at a particular potential in 400 MHz NMR (Bruker Avance DPX 400 MHz spectrometer). We have prepared NMR locking standard by adding 0.2 µl of DMSO as an internal standard in 1ml D_2O (for NMR locking). And obtaining the standardization curve (**Figure S13a**), we added 0.5 ml of aqueous solution with a known amount of 99.9% formic acid and 0.1 ml of NMR locking standard. In a typical NMR sample preparation, we have taken 0.5 ml of electrolyte solution with 0.1 ml of already prepared locking standard. Form ^1H NMR, in water suppression mode, we can quantitively estimate formate formation from the ratio of area under peak calculation with the help of a standardization curve. Finally, formate FE is calculated by the below equation –

$$FE_{Formate}(\%) = \frac{Q_{Formate}}{Q_{total}} \times 100\% = \frac{n_{Formate} \times N \times F}{j \times t} \times 100\%$$

Where, $n_{formate}$ is the amount of formate produced, N is the number of electrons transferred (2 for formate), and F is the Faradaic constant.

DFT Method:

DFT calculations were carried out following the Cambridge Serial Total Energy Package (CASTEP) code with the Perdew−Burke−Ernzerhof (PBE) functional and generalized gradient

approximation (GGA) as the exchange correlation (XC). The pseudopotential was taken as OTFG ultrasoft with 1350 eV as the cutoff of planewave basis. Also, Koelling–Hammon relativistic treatment was performed along with a 9 × 9 × 3 Monkhorst pack scheme grid. For geometry optimization, Broyden–Fletcher–Goldfarb–Shanno (BFGS) algorithm was used following the above-mentioned parameters along with $1e^{-6}$ eV as energy cutoff, 0.01 eVÅ^{-1} maximum force, $1e^{-4}$ Å as the maximum displacement, 0.01 GPa maximum stress and 1350 eV as the planewave cutoff. DFT slab models were employed for DFT calculation with a vacuum length of 15 Å to prevent interlayer interactions.[1] We have followed DFT + U method as described by Dudarev et al.[2] Since in CASTEP Hubbard U correction cannot be applied to sharing atom, we have used 3 × 3 × 3 super cell and the U_{eff} value was chosen following previous report.[3]

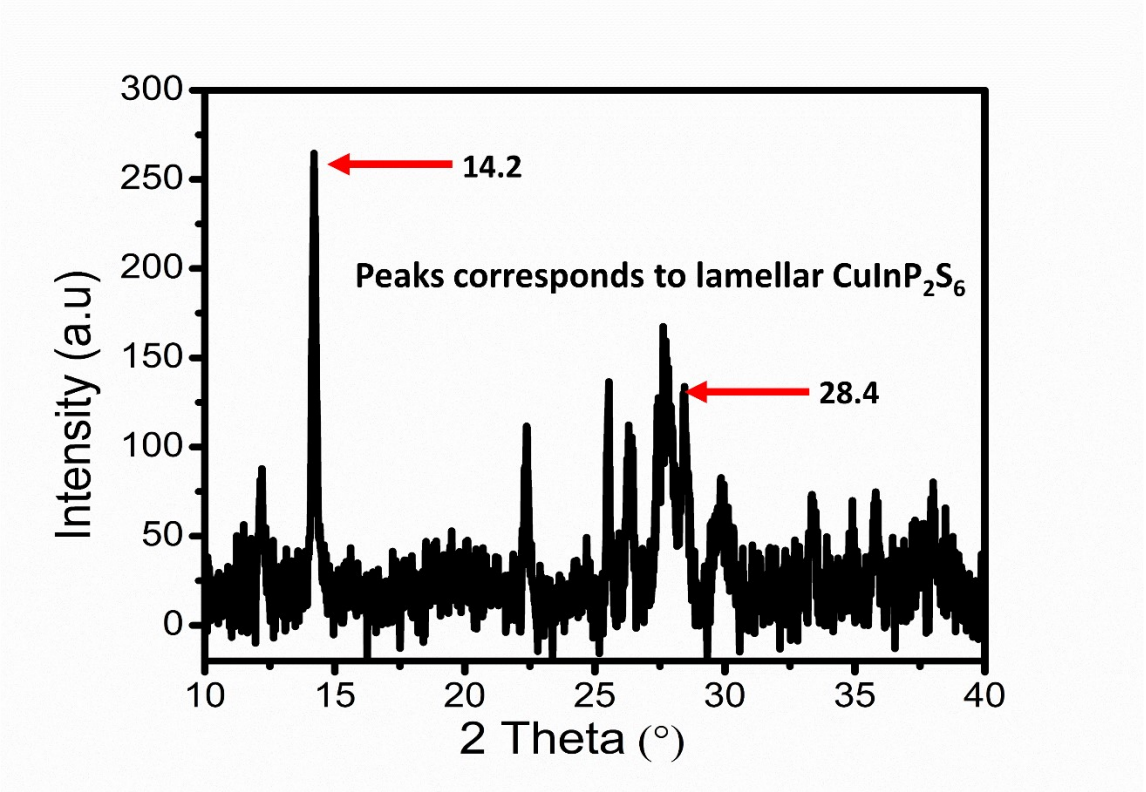

Figure S1: XRD of captured Intermediate containing 2D lamellar $CuInP_2S_6$

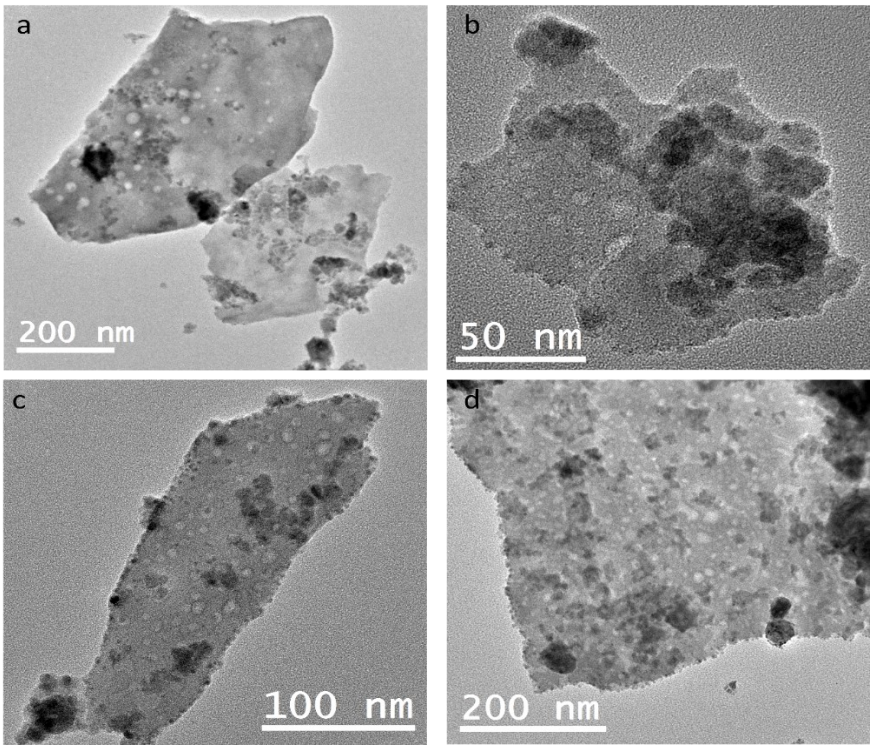

Figure S2: (a-d) TEM image of captured Intermediate containing 2D lamellar

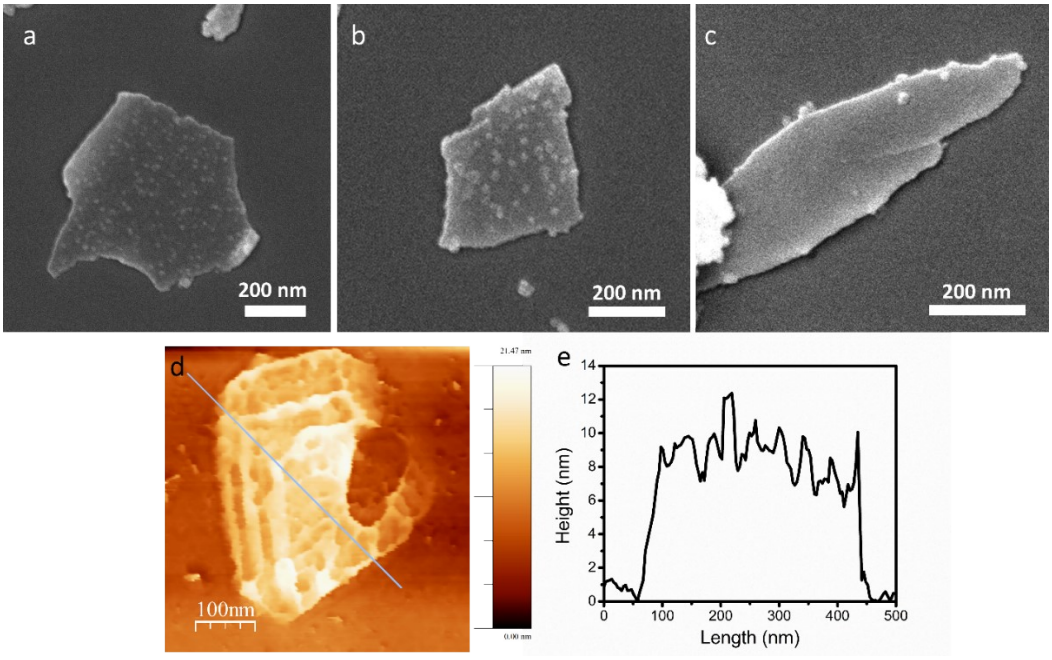

Figure S3: (a) SEM and (b) AFM data of captured Intermediate containing $CuInP_2S_6$ 2D lamella

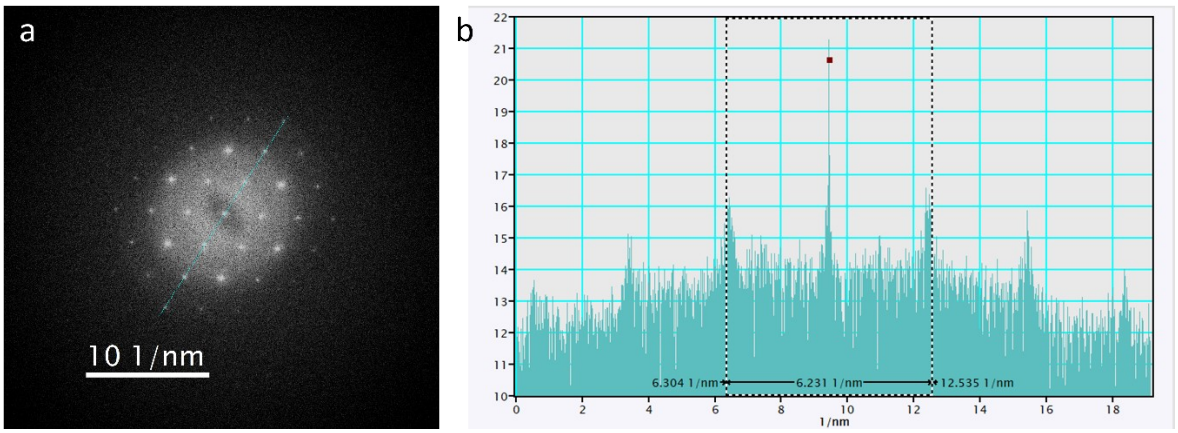

Figure S4: FFT and corresponding line profile analysis of HR-TEM data of P-doped CIS

Supplementary Note for Figure S4:

In the hexagonal FFT image, we have taken line scans, showing $2x(1/d_{hkl}) = 6.231\ nm^{-1}$. Again, from Bragg's law, $2d_{hkl}Sin\theta = n\lambda$ and putting n=1 and λ=0.154 nm, we found corresponding $2\theta = 27.76°$ which is the most intense XRD peak as shown in the Figure 2a corresponds to (111) facet.

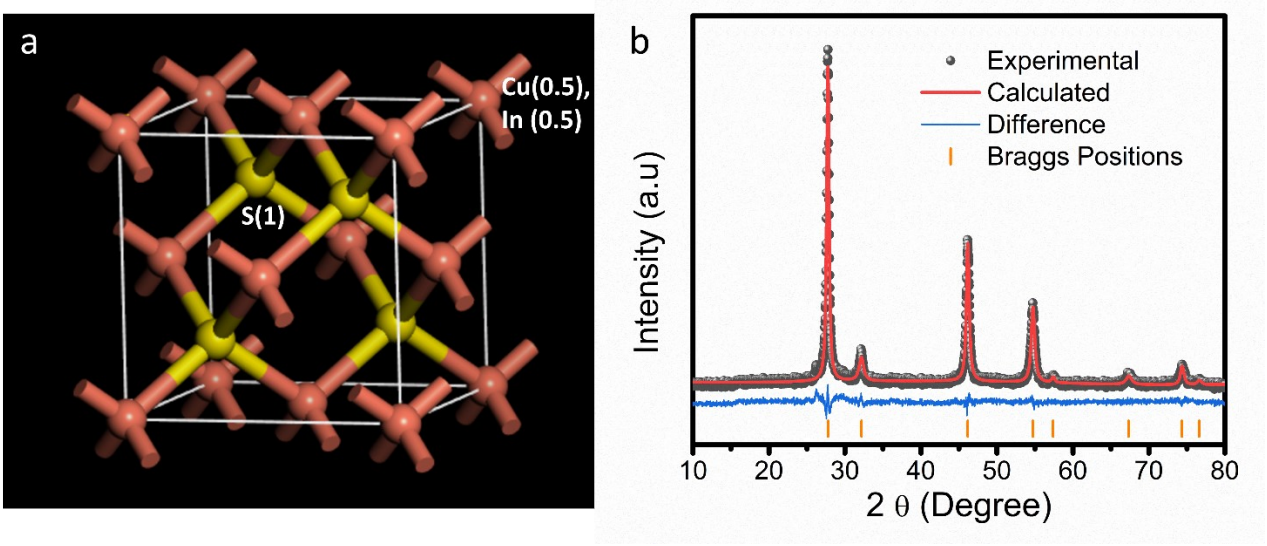

Figure S5: Zincblende structure and Rietveld Refinement of XRD data of P-doped CIS

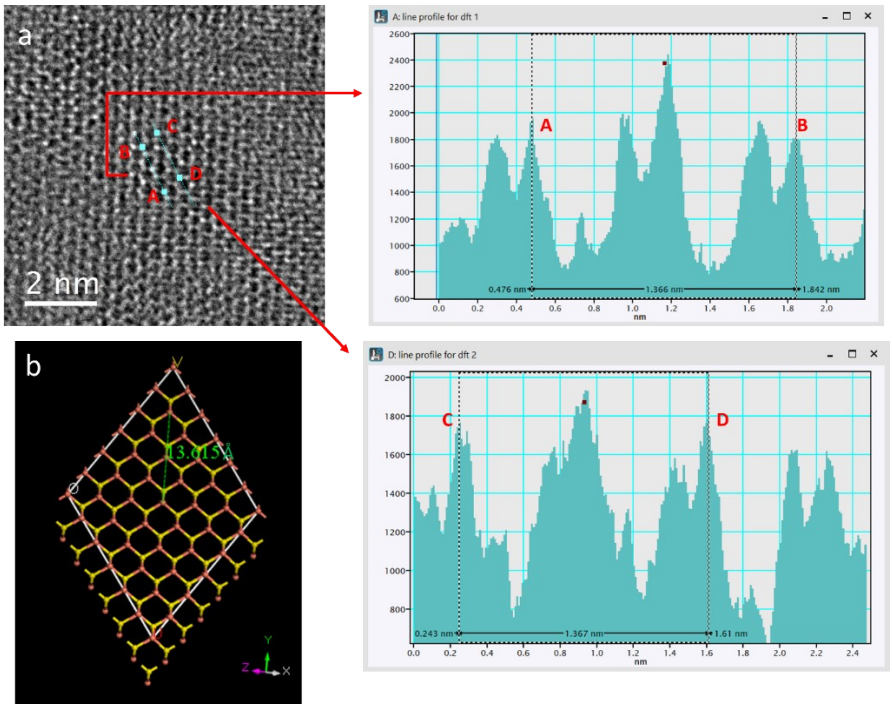

Figure S6: (a) HR-TEM line profiles showing Cu to 3rd Cu distance of the 2nd ring and (b) Showing same Cu to 3rd Cu distance of the 2nd ring in (111) facet cut after the Rietveld refined crystal structure (CIF file).

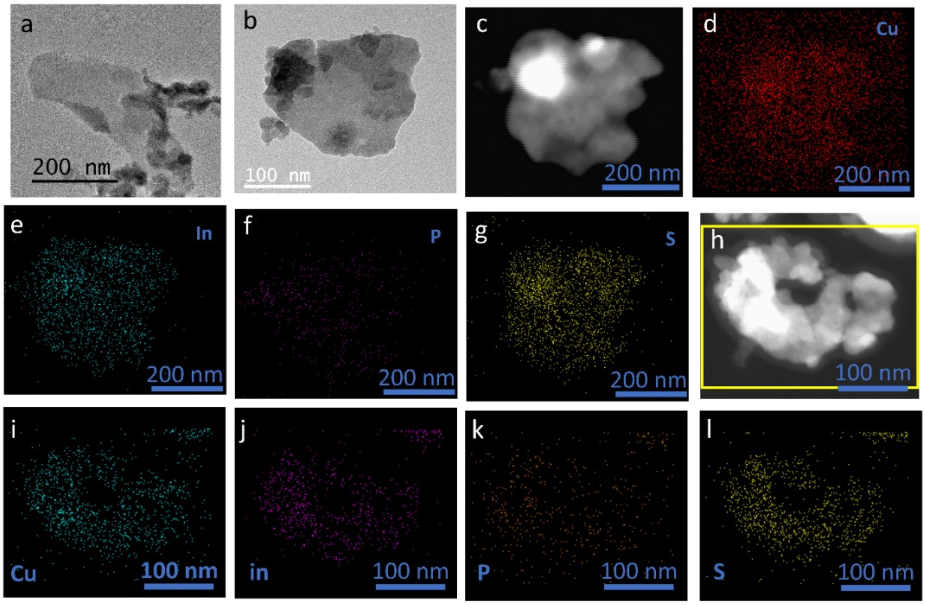

Figure S7: (a) additional TEM image of P-doped CIS; (b,c) Bright Field and HAADF TEM images, respectively and (d-g) showing elemental mapping on a Cu meshed TEM grid, resulting extra background signal in d; (h) HAADF TEM image and (i-l) presents corresponding elemental mapping on a Gold meshed TEM grid;

a

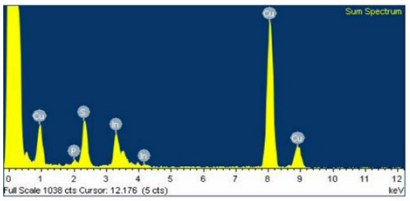

b

Element	Peak Area	Area Sigma	k factor	Abs Corrn.	Weight%	Weight% Sigma	Atomic%
P K	261	60	0.992	1.000	1.13	0.26	2.32
S K	2524	107	0.940	1.000	10.41	0.44	20.58
Cu K	10582	167	1.366	1.000	63.44	1.04	63.29
In L	3198	185	1.782	1.000	25.02	1.12	13.81
Totals					100.00		

c

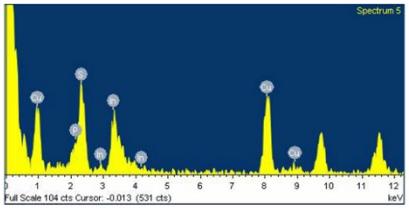

d

Element	Peak Area	Area Sigma	k factor	Abs Corrn.	Weight%	Weight% Sigma	Atomic%
P K	13	35	0.992	1.000	0.59	1.56	1.24
S K	419	50	0.940	1.000	17.71	2.19	45.88
Cu K	594	42	1.366	1.000	36.44	3.11	27.27
In L	565	84	1.782	1.000	45.26	4.05	25.61
Totals					100.00		

Figure S8: TEM EDX data- (a, b) High Cu atomic percentage is coming from the Cu meshed TEM grid. If we consider Cu:In=1:1 then, we can consider almost 50 % of Cu is coming from grid. Therefore, atomic doping percentage of phosphorus is almost 2.32*2 % i.e <5 %; (c, d) To further confirm the phosphorus doping and proper estimation of elemental distribution, we have repeated EDAX data on a Gold meshed TEM grid. Table d shows almost 1:1 Cu to In ratio (as assumed) with P doping <5 %.

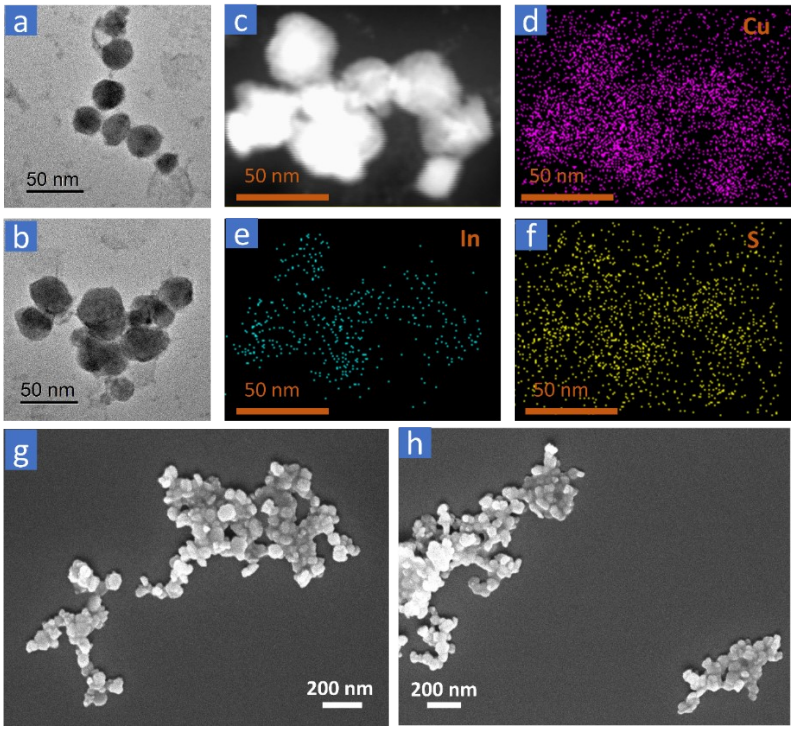

Figure S9: (a-b) TEM images; (c) HAADF TEM image; (d-f) corresponding elemental mapping and (g-h) SEM image of Wurtzite-CIS

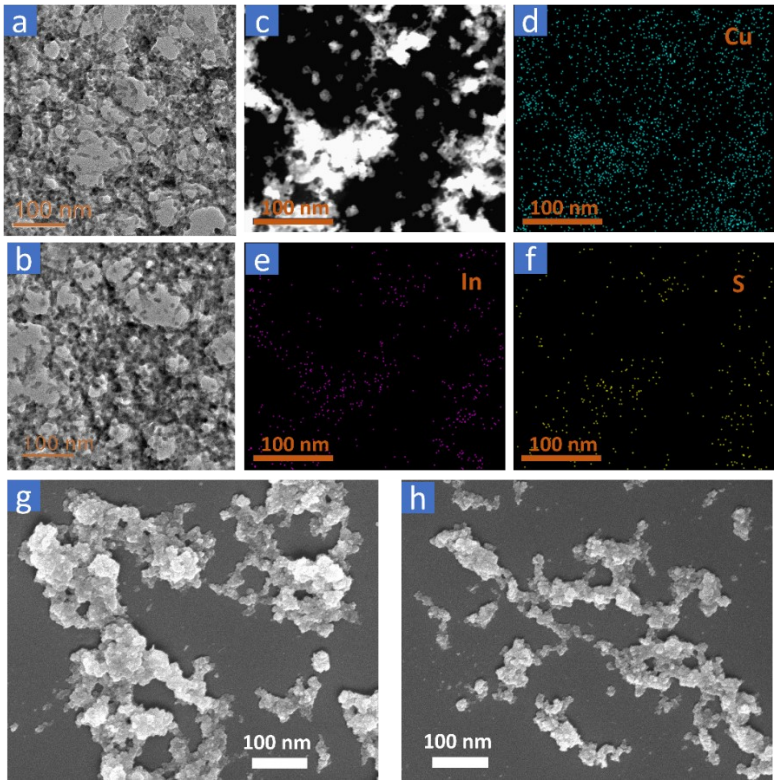

Figure S10: (a-b) TEM images; (c) HAADF TEM image; (d-f) corresponding elemental mapping and (g-h) SEM image of Zincblende-CIS

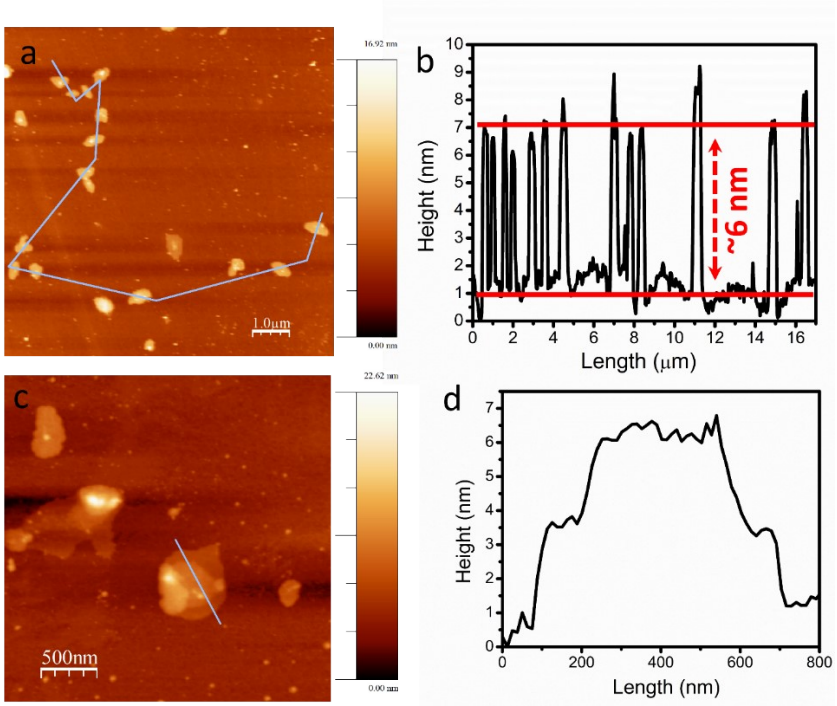

Figure S11: (a-b) AFM average height distribution and (c-d) additional AFM image showing stacking of 2D flakes

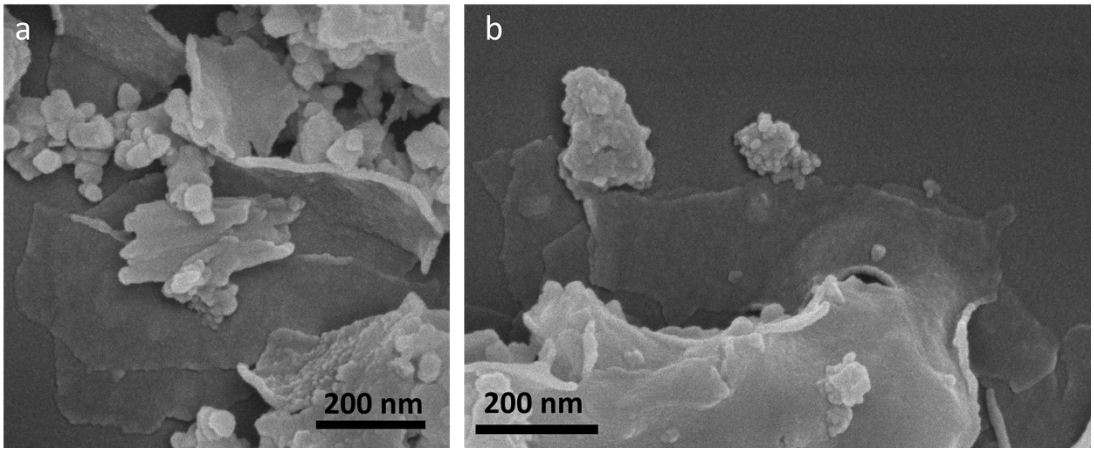

Figure S12: additional SEM data of P-doped $CuInS_2$

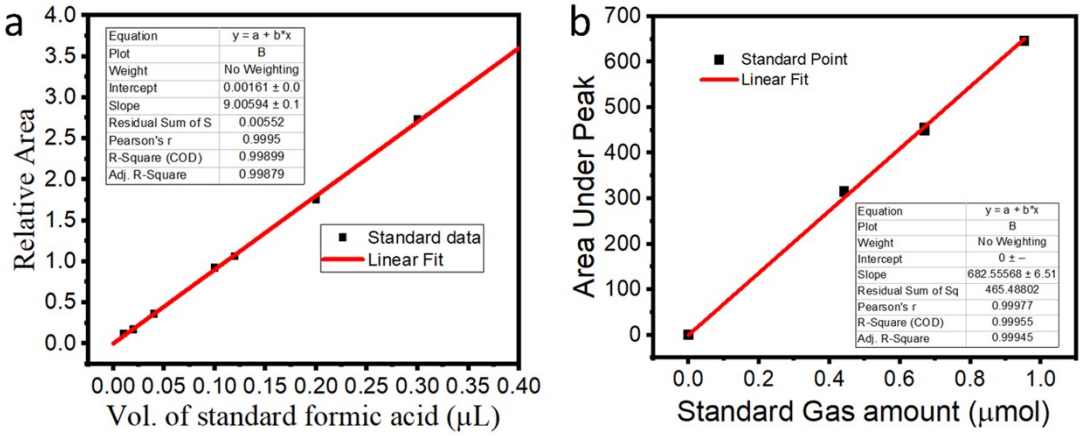

Figure S13: (a) Formate calibration curve for NMR; (b) CO calibration curve for GC

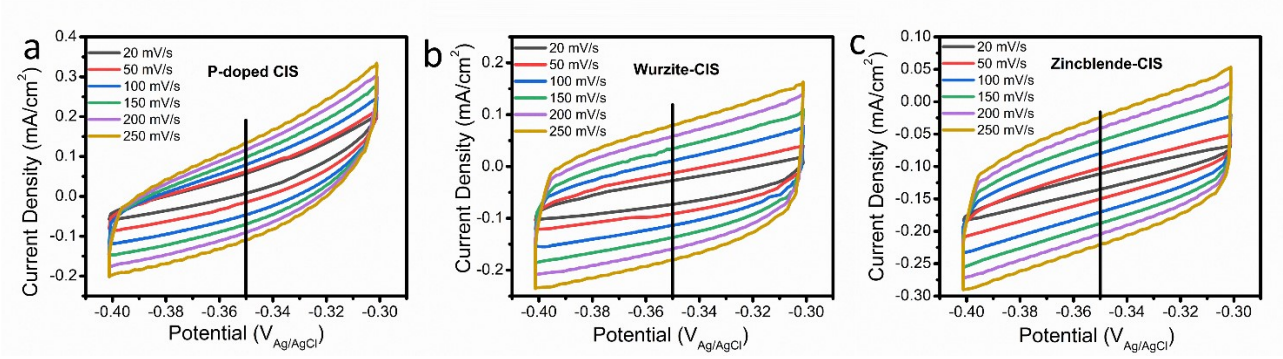

Figure S14: Cyclic voltammetry study at non faradaic region of (a) P-doped CIS; (b) Wurtzite-CIS; (c) Zincblende-CIS

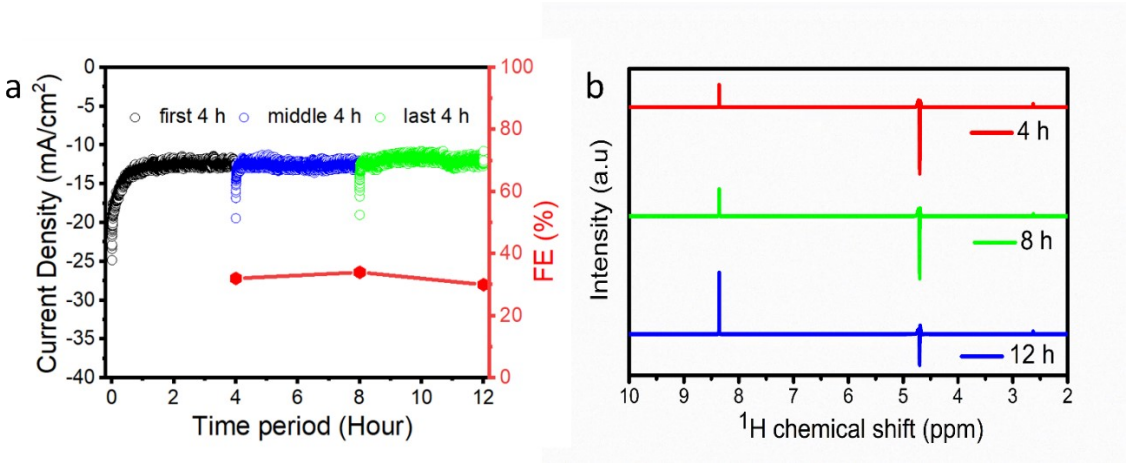

Figure S15: (a) long term stability test with FE; (b) Corresponding product analysis via NMR

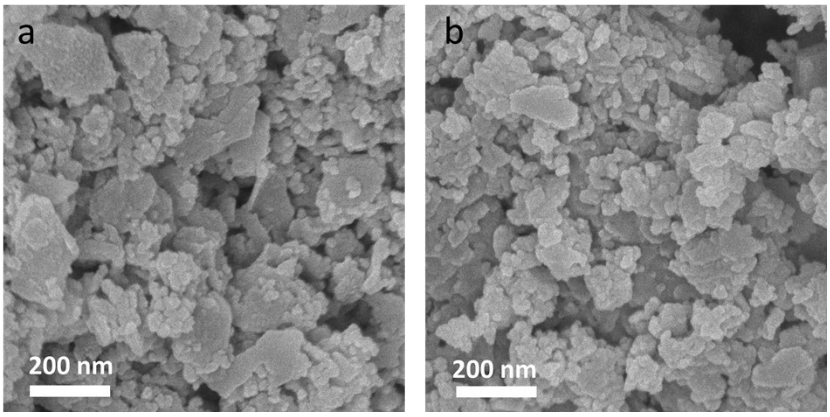

Figure S16: SEM images of the P doped CIS electrode after 1h chronoamperometry

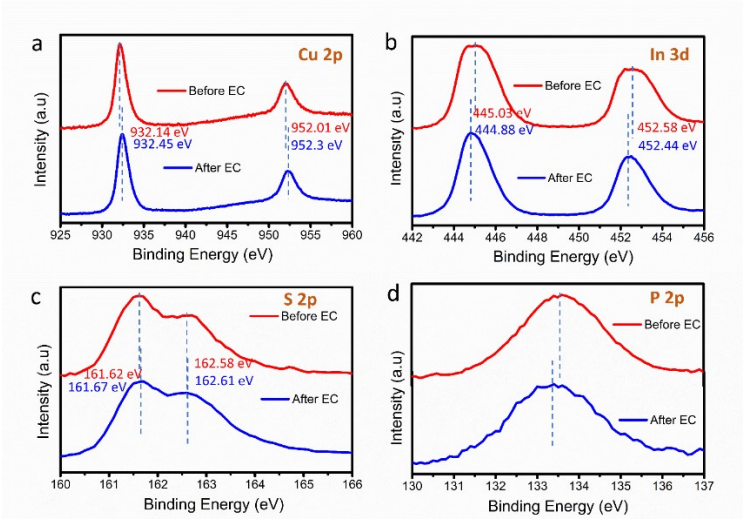

Figure S17: XPS overlay plot of P-doped CIS Before (red line) and After 1 h electrolysis (blue line) showing the core levels of (a)Cu 2p; (b)In 3d; (c) S 2p and (d) P 2p, respectively

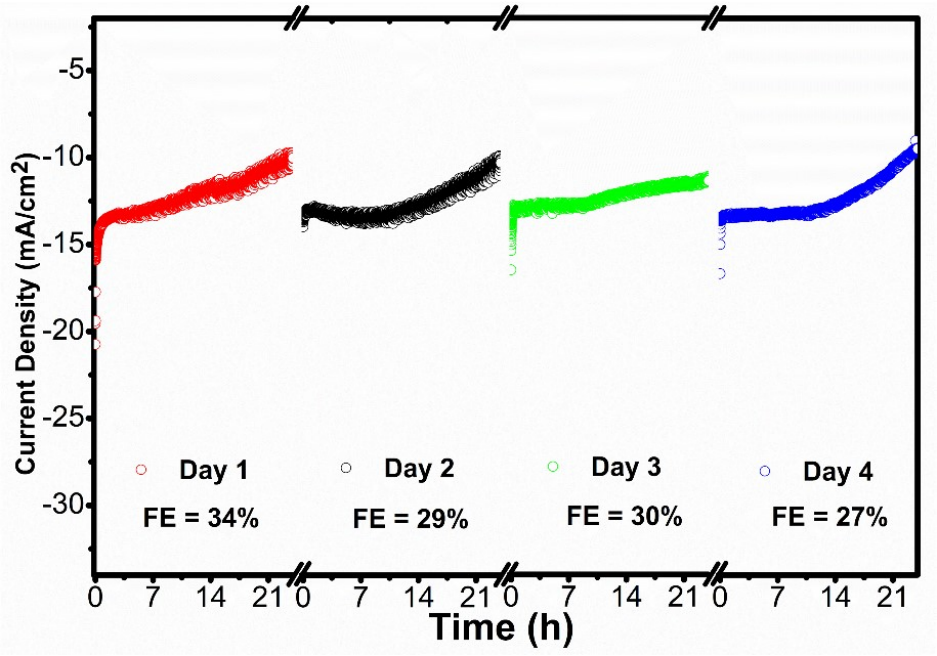

Figure S18: Four day long cyclic stability test

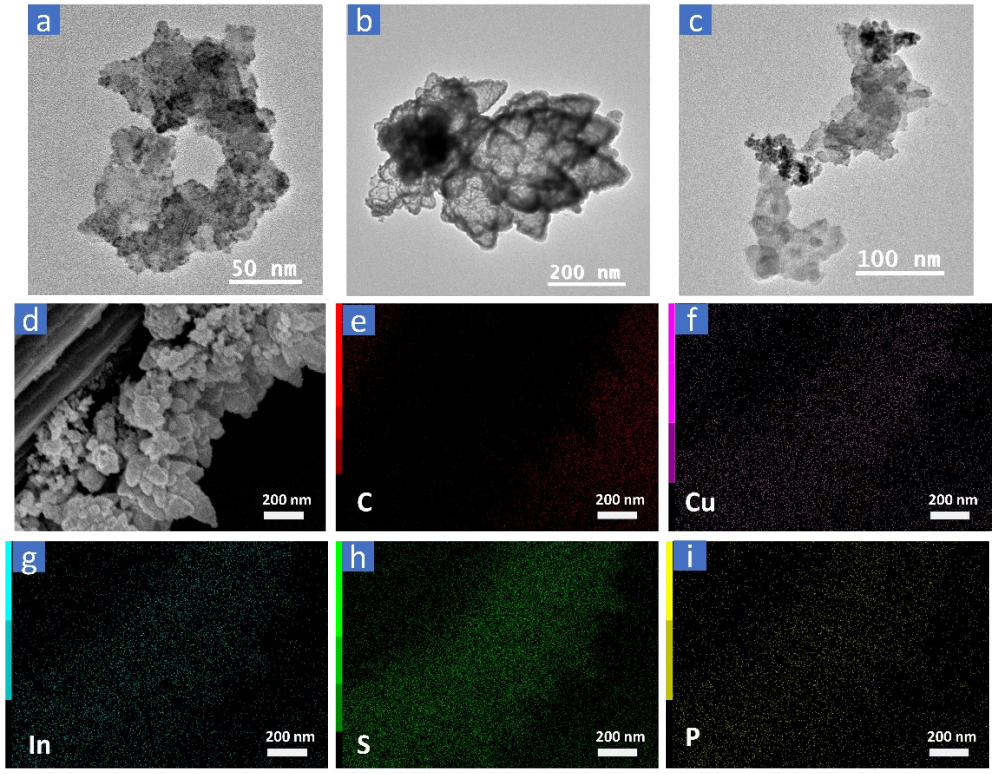

Figure S19: After 4-day long stability test (a-c) TEM images; (d) SEM image of electrode and (e-i) corresponding elemental mapping

Table S1: Comparison of formate Faradaic efficiency (FE), partial current density, applied potential, and electrolyte conditions for representative state-of-the-art electrocatalysts for electrochemical CO_2 reduction to formate in H-type cells with neutral bicarbonate electrolytes. Data for P-doped 2D CIS from this work is included for direct benchmarking.

Entry No.	**Materials**	**Formate FE (%) [main product]**	**Current density (mA mA/cm²) at Potential (V_{RHE})**	**Stability (h)**	**Scalability of catalyst with reproducibility**	**Reference No.**
1	2D Zincblende (111) $CuInS_2$	40.2	**-13.5 at -0.84**	**4 cycles of 24h**	**High** (one pot wet chemical synthesis)	This Work
	Non 2D Zincblende $CuInS_2$	34.5				
	Non 2D Wurtzite $CuInS_2$	28.5				
2	$CuInO_2$	31 [CO]	-1.67 at -0.7	5h	Average (multi step)	[4]
	Cu_2O	10 [CO]	-1.67 at …			
3	CuIn (In at 80%)	**62**	-1.5 at -1	10h	Very low (electrodeposition)	[5]
	CuIn (In at 40 and 60%)	50				
4	C−Cu/In_2O_3-1.5	~45 [Syn gas]	At -0.8	--	Low (multi step)	[6]
	C−Cu/ In_2O_3-0.8	~20 [Syn gas]	At -0.8	--	Low (multi step)	
	C−Cu/ In_2O_3-0.4	~8 [Syn gas]	At -0.8	5h (-8 at -0.7)	Low (multi step)	
5	V-doped In_2O_3	**~70**	-5.5 at -1.17	--	**High** (wet chemical synthesis)	[7]
6	Cu-SnO_2	5 [EtOH]	-4.5 at -0.6	14h	Average	[8]
	Cu_2O-SnO_2	10 [C_2H_4]	-4.0 at 0.6	14h	Average	
7	Sn/N-doped Carbon	**63**	**-16.6 at -0.6**	24h	Average	[9]

	Atomically Dispersed Sn/N-doped carbon	nil	-1.5 at -0.6	24h	Low (multi step)	
8	Patterned Cu-Sn	26.8 [CO]	-2.57 at -1 (calculated from table S2)	10h	Low (multi step)	[10]
9	Au1Sn2 Au1Sn4	42 51	-11 at -1.1 At -0.9	10h (-8 at -1)	Low (tough to reproduce)	[11]
10	SnO_2/C hollow sphere	64-49	-5.5 at -0.9	12h	Low (multi step)	[12]
11	CuSn NW/C-air CuSn NW/C-H_2 CuSn NW/C-N_2	**90.2** 62.6 59.9	**-17.33** at -1	10h	Low (multi step) Low (multi step) Low (multi step)	[13]
12	Cu-5Sn-30 Cu-30Sn-10	~45 [Syn gas] ~15 [Syn gas]	-2.5 at -0.9 -3.2 at -0.9	10h 10h	Very low (electrodeposition)	[14]

References:

1 K. Roy, D. Ghosh, S. Maitra and P. Kumar, *J. Mater. Chem. A*, 2023, **11**, 21135–21145.

2 S. L. Dudarev, G. A. Botton, S. Y. Savrasov, C. J. Humphreys and A. P. Sutton, *Phys. Rev. B*, 1998, **57**, 1505–1509.

3 K. Bhola, J. J. Varghese, L. Dapeng, Y. Liu and S. H. Mushrif, *J. Phys. Chem. C*, 2017, **121**, 21343–21353.

4 A. Jedidi, S. Rasul, D. Masih, L. Cavallo and K. Takanabe, *J. Mater. Chem. A*, 2015, **3**, 19085–19092.

5 Z. B. Hoffman, T. S. Gray, K. B. Moraveck, T. B. Gunnoe and G. Zangari, *ACS Catal.*, 2017, **7**, 5381–5390.

6 H. Xie, S. Chen, F. Ma, J. Liang, Z. Miao, T. Wang, H. L. Wang, Y. Huang and Q. Li, *ACS Appl. Mater. Interfaces*, 2018, **10**, 36996–37004.

7 M. G. Kim, J. Jeong, Y. Choi, J. Park, E. Park, C. H. Cheon, N. K. Kim, B. K. Min and W. Kim, *ACS Appl. Mater. Interfaces*, 2020, **12**, 11890–11897.

8 H. Liu, C. Yang, T. Bian, H. Yu, Y. Zhou, Y. Zhang and L. Sun, *Adv. Energy Mater.*, 2025, **15**, 1–11.

9 Y. Zhao, J. Liang, C. Wang, J. Ma and G. G. Wallace, *Adv. Energy Mater.*, 2018, **20**, 2307862.

10 C. J. Yoo, W. J. Dong, J. Y. Park, J. W. Lim, S. Kim, K. S. Choi, F. O. Odongo Ngome, S. Y. Choi and J. L. Lee, *ACS Appl. Energy Mater.*, 2020, **3**, 4466–4473.

11 A. M. Ismail, G. F. Samu, Á. Balog, E. Csapó and C. Janáky, *ACS Energy Lett.*, 2019, **4**, 48–53.

12 Yiliguma, Z. Wang, C. Yang, A. Guan, L. Shang, A. M. Al-Enizi, L. Zhang and G. Zheng, *J. Mater. Chem. A*, 2018, **6**, 20121–20127.

13 J. Wang, Y. Ji, Q. Shao, R. Yin, J. Guo, Y. Li and X. Huang, *Nano Energy*, 2019, **59**, 138–145.

14 A. R. Woldu, K. Harrath, Z. Huang, X. Wang, X. Huang, D. Astruc and L. Hu, *Small*, 2024, **20**, 2307862